Predissociation in the $B\,^1\Pi_u$ state of $^6Li^7Li$: Accidental perturbations beyond the ungerade-gerade symmetry breaking

P. Cacciani*
Laboratoire PhLAM, Université de Lille 1, 59655 Villeneuve d'Ascq Cedex, France

V. Kokoouline
Department of Physics and JILA, University of Colorado, Boulder, Colorado, 80309-0440, USA

N. Bouloufa, F. Masnou-Seeuws, and R. Vetter
Laboratoire Aimé Cotton, Bâtiment 505, Campus d'Orsay, 91405 Orsay Cedex, France
(Received 4 April 2003; published 22 October 2003)

Recently, an unusual predissociation was observed for some vibrational levels of the $B\,^1\Pi_u$ molecular state of $^6Li^7Li$ [Bouloufa *et al.*, Phys. Rev. A **63**, 042507 (2001)]. It was interpreted as due to the *ungerade-gerade* symmetry breaking that couples the $B\,^1\Pi_u$ quasibound levels to the $1\,^1\Pi_g$ continuum. However, the agreement between theory and experiment was not perfect for predissociation rates of three rovibrational levels, occurring for isolated quantum numbers. Here, we identify these additional perturbations as due to the rotational coupling of the $1\,^1\Pi_g$ continuum with quasibound levels of the $2\,^1\Sigma_g^+$ state. In addition, our method allows a calculation of the Λ-doubling in the $1\,^1\Pi_g$ state and dissociation rates of quasibound $2\,^1\Sigma_g^+$ levels for three isotopomers of Li_2. Comparison with experimental data is discussed.

DOI: 10.1103/PhysRevA.68.042506 PACS number(s): 33.20.Wr, 33.20.Sn, 33.80.Gj

I. INTRODUCTION

For alkali dimers, the $B\,^1\Pi_u$ state that converges to the first excited asymptote $(ns+np)$ exhibits a barrier to dissociation. Dissociation by tunneling has been observed for Li_2 [1], Na_2 [2], K_2 [3,4], and Rb_2 [5]. Recently, unexpectedly high predissociation rates of some $B\,^1\Pi_u$ vibrational levels were observed in the $^6Li^7Li$ molecule [6]. Tunneling effects were too small to explain these rates, which were attributed to the *ungerade-gerade* symmetry breaking, which occurs only in the $^6Li^7Li$ isotopomer. After the first experimental detection of the effect, showing only a couple of unexpected predissociation rates, a theoretical model was developed. It was suggested that these high predissociation rates are caused by a coupling between quasidiscrete vibrational levels of the $B\,^1\Pi_u$ state with the vibrational continuum of the $1\,^1\Pi_g$ state. Since the *ungerade-gerade* symmetry is not perfect in $^6Li^7Li$, this coupling is not strictly zero. The effect is very small and the coupling was treated as a perturbation leading to a calculation of predissociation rates for different rovibrational levels of the molecule. In these calculations, the Fourier grid method [7–10] with an absorbing potential was employed. For a fixed vibrational level v and various rotational quantum numbers J, the calculated predissociation rates exhibit an oscillating behavior vs rotational energy. It is linked to oscillations of the Franck-Condon factor between the $B\,^1\Pi_u$ quasidiscrete vibrational levels and those of the $1\,^1\Pi_g$ continuum. Later, systematic measurements were carried out [11], confirming almost perfectly the proposed model and the predicted rates. However, there were few measured rates, which could not be interpreted in a framework of the proposed model. These discrepancies occur for three rotational quantum numbers and for the *e*-parity component only. As an example, the dissociation rate, measured for $(v=8, J_e=48)$, is three times larger than the calculated one, whereas the agreement is good for all neighboring values of J. In this work, we explore the origin of these additional perturbations and we interpret them as due to an indirect coupling between quasidiscrete levels of the $B\,^1\Pi_u$ state and those of the $2\,^1\Sigma_g^+$ state, which also displays a potential barrier and dissociates to $(2s+2p)$. Completing our previous theoretical model, where the $B\,^1\Pi_u$ levels are coupled by a u-g symmetry breaking term to the continuum of the $1\,^1\Pi_g$ state, we now include the known rotational coupling of this continuum with the $2\,^1\Sigma_g^+$ levels. The potentials of the three states are shown in Fig. 1.

The paper is organized as follows. In Sec. II, we describe briefly the experimental setup, focusing on the technique employed to measure the predissociation rates, and we recall the three anomalous data points. Then, in Sec. III we present a model treating the coupling of the three molecular states. In Sec. IV we discuss results of the calculation and compare to the experimental measurements. We also present the calculation of the Λ-doubling for the $1\,^1\Pi_g$ state, and we compare results with previous measurements [16]. Finally, a conclusion is exposed in Sec. V.

II. EXPERIMENTAL SETUP: OBSERVED PERTURBATIONS

The sub-Doppler experiment is based on a molecular effusive beam of lithium crossed at a right angle by a cw tunable dye laser oscillating around 460 nm, the total laser-induced fluorescence being collected vs the laser frequency. Narrow absorption profiles ($\simeq$65 MHz full width at half maximum) are then recorded and calibrated using Fabry-

*Electronic address: Patrice.Cacciani@univ-lille1.fr

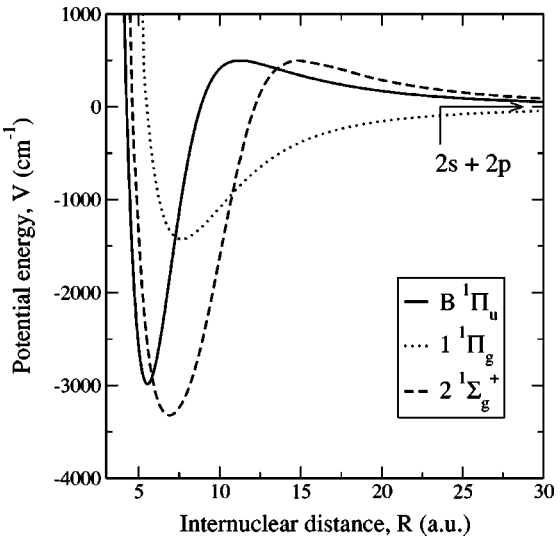

FIG. 1. The Li_2 potential curves involved in unexpected predissociation observed in $^6Li^7Li$. The $B\,^1\Pi_u$ molecular state (solid line) [12] and the $2\,^1\Sigma_g^+$ molecular state (dashed line) [13–15] have both potential barriers. The barriers allow an existence of several vibrational levels whose energies are above the dissociation limit $(2s+2p)$. No direct coupling exists between these two molecular states, but they are both coupled to the $1\,^1\Pi_g$ state (dotted line) [16] by the *u-g* symmetry-breaking term and the rotational coupling term $(J^+L^-+J^-L^+)$, respectively. Since the intermediate $1\,^1\Pi_g$ state exhibits no barrier for $J=0$, it possesses only a continuum vibrational spectrum above the dissociation limit. Measurable perturbations occur on predissociation of quasibound levels of the $B\,^1\Pi_u$ and $2\,^1\Sigma_g^+$ states when they coincide in energy.

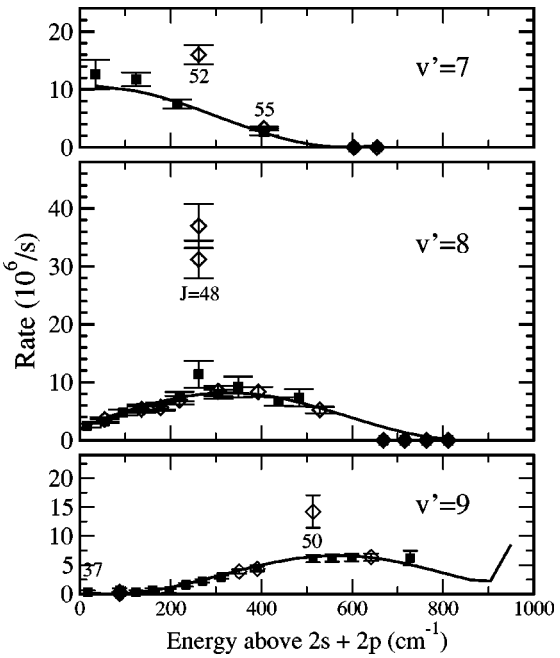

FIG. 2. Dissociation rates of the series $v=7$, 8, and 9 vs *J*. Filled squares are experimental data for *f*-parity, and open diamonds are for *e*-parity data. The curves represent rates calculated using the *u-g* symmetry breaking model. The agreement is very good, except for three levels of the $B\,^1\Pi_u$ states $(v=7,J_e=52)$, $(v=8,J_e=48)$, and $(v=9,J_e=50)$.

Perot fringes and the tellurium absorption spectrum [17].

Predissociation is investigated in two ways: measurement of spectral broadening when the dissociation rate is high enough to be detected (>10 MHz) and detection of the atomic $(2p\rightarrow 2s)$ fluorescence, which occurs after dissociation of the excited $B\,^1\Pi_u$ level above the $2p+2s$ asymptote. In the latter technique, we are able to distinguish the molecular fluorescence, which is emitted into many vibrational states of the $X\,^1\Sigma_g^+$ ground state, from the atomic one at 671 nm. This is achieved by using different colored filters in the light detection system. A first frequency scan (a) is performed with a yellow filter, which collects a maximum of the fluorescence, cutting only the laser stray light. A second scan (b) is performed with a red filter, which transmits only the atomic fluorescence. The lines present in this latter (b) spectrum represent transitions connected to predissociated levels. Comparing the intensities of the two spectra, we can measure the branching ratio ρ between dissociation and fluorescence. More precisely, we measure

$$\rho=\frac{I_a}{I_b}=\frac{(\alpha A+k)}{k}, \tag{1}$$

where *A* is the spontaneous transition probability of the *B* state, α is the fraction of the molecular fluorescence transmitted to the light detector through the yellow filter, and *k* is the dissociation rate. This equation is valid assuming an equivalent transmission of the two filters at 671 nm, and a nearly constant quantum efficiency of the detector over the visible spectral range. The parameter α can be easily estimated from the knowledge of Franck-Condon factors and from the transmission curve of the yellow filter. Figure 1 of Bouloufa *et al.* [11] shows an example of such spectra. This technique allowed measurements of low dissociation rates for nine vibrational series, in the range 0.3×10^6 s^{-1}–40×10^6 s^{-1}, much lower than the radiative rate of 110×10^6 s^{-1}. For such values, detecting a spectral broadening is almost impossible. Thus, the selective detection of atomic fluorescence is a key point to put into evidence the breaking of the *u-g* symmetry for $^6Li^7Li$.

A symmetry-breaking model was invoked, introducing a coupling term h_{ug} to the Hamiltonian of the $^6Li^7Li$ molecule. This term is not zero for $^6Li^7Li$ because the center of mass of the molecule does not coincide with the center of molecular symmetry. Since the ''defect'' of symmetry is small, the term h_{ug} was treated in a perturbative way. A Schrödinger equation including h_{ug} was solved using the mapped Fourier grid method. An approximate coupling strength was first evaluated at the infinite internuclear separation, where the coupling is responsible for the isotopic shift of the $2p\rightarrow 2s$ atomic transition at 671 nm. Then the coupling was fitted to experimental data. By adjusting only one parameter, we were able to reproduce all the experimental data (Fig. 2), except for three values of (v,J_e), which were far outside experimental error bar. This requires a theoretical explanation.

III. THEORETICAL MODEL AND CALCULATION

The accidental character of observed perturbations in the $B\,^1\Pi_u$ spectrum suggests [6] an interaction with quasibound levels rather than with a continuum. In addition to $B\,^1\Pi_u$, there is only one molecular state, $2\,^1\Sigma_g^+$, dissociating to the $2s+2p$ asymptote, which has a potential barrier at $J=0$. The barrier is high enough to support several quasibound vibrational levels for values of J as high as 80. For all other molecular potential curves converging to the same asymptote, there is no barrier at $J=0$, and the attractive curves are such that in the range of rotational levels considered here, the centrifugal term is not strong enough to create a barrier. Therefore, the $2\,^1\Sigma_g^+$ state is the only possible candidate (dashed line in Fig. 1). This hypothesis is consistent with the fact that the perturbations are observed only for e-parity $B\,^1\Pi_u$ levels. No direct coupling exists between $B\,^1\Pi_u$ and $2\,^1\Sigma_g^+$ states. However, both states are coupled to the continuum of the $1\,^1\Pi_g$ state. The $B\,^1\Pi_u$ state is coupled to $1\,^1\Pi_g$ by the u-g symmetry-breaking coupling, discussed in the Introduction, whereas the $2\,^1\Sigma_g^+$ state is coupled to $1\,^1\Pi_g$ by the familiar rotational coupling operator $-1/(2\mu R^2)(J^+L^- + J^-L^+)$ [18]. The effect of such a coupling has been frequently observed between bound states with $\Delta\Lambda = \pm 1$, where Λ is the projection of the electronic angular momentum on the molecular axis. It leads, for example, to Λ-doubling shifts for Π states. Here, we consider the coupling between the vibrational continuum of the $1\,^1\Pi_g(e)$ state with $2\,^1\Sigma_g^+$ quasibound levels or, from the other side, the predissociation of these levels towards the $1\,^1\Pi_g(e)$ continuum.

Thus, vibrational levels of $B\,^1\Pi_u$ and $2\,^1\Sigma_g^+$ states can weakly interact. The effect is very small and can in principle be only observed only when a $B\,^1\Pi_u$ vibrational level approaches very closely in energy to a $2\,^1\Sigma_g^+$ level. The effect is stronger for large rotational quantum numbers J, since the rotational coupling increases linearly with J values. An experimental confirmation arises from the fact that the perturbations are observed only for high J. A second confirmation comes from a comparison of energies of $B\,^1\Pi_u$ and $2\,^1\Sigma_g^+$ levels. Energies of the $B\,^1\Pi_u$ levels are very well known from the experiment. The situation is different for the $2\,^1\Sigma_g^+$ levels. Experimentally, they were first observed by Fourier-transform spectroscopy, by excitation of the $B\,^1\Pi_u$ levels, which relax towards the $2\,^1\Sigma_g^+$ state by inelastic collisions [14]. The vibrational levels were observed up to $v=16$ and an Rydberg-Klein-Rees (RKR) potential curve was obtained for the bottom of the potential. Later, a near-infrared, two-photon laser experiment [15] allowed the direct excitation of the vibrational levels up to $v=21$. Therefore, the knowledge of the potential curve remains limited by energies less than 400 cm^{-1} below the dissociation energy. Consequently, no quasibound $2\,^1\Sigma_g^+$ levels have been observed experimentally, and further knowledge relies necessarily on *ab initio* calculations [13]. For our study, we joined the accurate RKR potential curve smoothly to the *ab initio* curve in order to describe the whole potential. It implies that energies of the quasibound $2\,^1\Sigma_g^+$ levels are reproduced with limited accuracy.

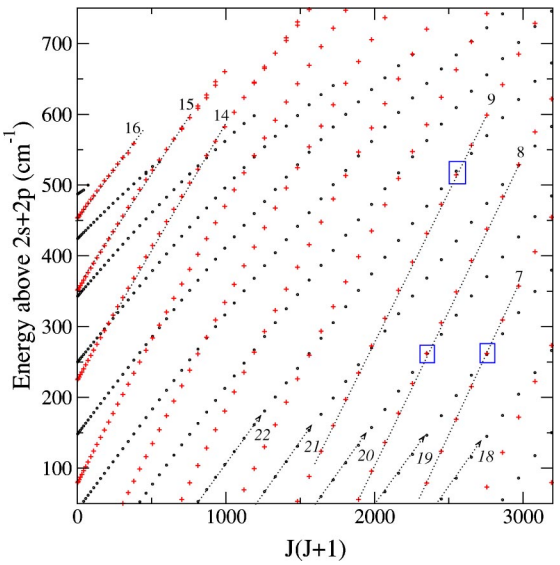

FIG. 3. Diagram of rovibrational energies of the $B\,^1\Pi_u$ (crosses) and $2\,^1\Sigma_g^+$ (circles) molecular states. Roman and italic numbers enumerate vibrational series v of the $B\,^1\Pi_u$ and $2\,^1\Sigma_g^+$ levels, respectively. Three levels (in small rectangles) of the $B\,^1\Pi_u$ state ($v=7, J=52$), ($v=8, J=48$), and ($v=9, J=50$) are perturbed by three close levels of the $2\,^1\Sigma_g^+$ state. The diagram suggests that there could be more perturbations, which have not been observed experimentally.

Figure 3 gives energies of $B\,^1\Pi_u$ and $2\,^1\Sigma_g^+$ molecular levels as a function of the quantity $J(J+1)$. For a fixed value of v, they are almost linear functions of $J(J+1)$. Rotational series of the $B\,^1\Pi_u$ state are represented by almost parallel lines for each v (roman number), whereas rotational series of the $2\,^1\Sigma_g^+$ state are represented by another set of parallel lines with a different inclination to the abscissa axis (italic number). Crossing points between the two sets of rotational series are possible candidates to produce perturbations if the abscissa of a crossing point is close to $J(J+1)$ values with integer J. Small rectangles in Fig. 3 show positions of the $B\,^1\Pi_u$ rovibrational levels for which abnormal predissociation rates were observed: ($v=7, J_e=52$), ($v=8, J_e=48$), and ($v=9, J_e=50$). As one can see in Fig. 3, the rotational series of the $B\,^1\Pi_u$ levels cross with the $2\,^1\Sigma_g^+$ series near these specified positions, respectively, with ($v'=19, J=52$), ($v'=20, J=48$), and ($v'=22, J=50$) levels. However, the coincidence is not good for the ($B\,^1\Pi_u, v=9, J=50$) level, most likely, because of a poor accuracy of the $2\,^1\Sigma_g^+$ potential curve in the energy range of 500 cm^{-1} above the dissociation limit. The above analysis also gives some insight where other possible perturbations could occur. Below we give a quantitative approach to describe the effect on the predissociation rates of the $B\,^1\Pi_u$ levels.

In order to treat this effect quantitatively, we solve the Schrödinger equation for vibrational motion in the three-state potential of Li_2. For the solution, we employ the mapped Fourier grid method with an absorbing potential as described in Refs. [6,11]. Vibrational wave functions in the channels $B\,^1\Pi_u$ and $2\,^1\Sigma_g^+$, and the continuum wave function in the channel $1\,^1\Pi_g$ are represented by an expansion on a Fourier

grid of $N=305$ points typically. An absorbing imaginary potential is placed at the end of the grid in order to absorb dissociating flux. Complex eigenvalues are obtained by diagonalization of a $3N\times 3N$ matrix. The real part of energies yields the energies of the levels, and the imaginary part gives their half-widths. From the latter, the predissociation rate is computed as described in Ref. [11]. The Hamiltonian of the considered system is written as

$$\hat{H}=-\frac{1}{2\mu}\frac{d^2}{dR^2}+\hat{V}(R)+\frac{J(J+1)-\Omega^2}{2\mu R^2}, \tag{2}$$

where Ω is the projection of the total angular momentum on the molecular axis. It coincides with the projection of the orbital electronic momentum on the axis. Ω is 0 or 1. The coupling h_{ug} between $B\,^1\Pi_u$ and $1\,^1\Pi_g$ is the same as in Ref. [11] with no direct coupling between $B\,^1\Pi_u$ and $2\,^1\Sigma_g^+$. The coupling between $1\,^1\Pi_g$ and $2\,^1\Sigma_g^+$ is a rotational coupling term $b\sqrt{J(J+1)}/(2\mu R^2)$ [16], where b is given by

$$b=\sqrt{2}\langle\,^1\Pi|L^+|\,^1\Sigma^+\rangle=\sqrt{2}\sqrt{L(L+1)}. \tag{3}$$

The factor $\sqrt{2}$ arises when the basis set is changed from the degenerate set, $^1\Pi$ $\Lambda=\pm 1$, to the one with states $^1\Pi_e$, $^1\Pi_f$. As the states $2\,^1\Sigma_g^+$ and $1\,^1\Pi_g$ dissociate to Li$(2s)$ $+$Li$(2p)$, we have $L=1$, giving $b=2$. Thus, the complete potential is represented by a 3×3 R-dependent matrix:

$$\hat{V}=\begin{pmatrix} V_{^1\Pi_u}(R) & h_{ug} & 0 \\ h_{ug} & V_{^1\Pi_g}(R) & \dfrac{b\sqrt{J(J+1)}}{2\mu R^2} \\ 0 & \dfrac{b\sqrt{J(J+1)}}{2\mu R^2} & V_{^1\Sigma_g^+}(R) \end{pmatrix}. \tag{4}$$

The accuracy of calculated energies and dissociation rates in the mapped Fourier method is controlled by a parameter β [9]. In the present calculation, this parameter is chosen to be 0.6. It provides a relative error in determination of energies of low bound levels about $10^{-8}\sim 10^{-9}$ (absolute error is 10^{-4}–10^{-5} cm^{-1}). The accuracy of excited and predissociated levels is worse, about 0.01 cm^{-1}. The poor accuracy of these levels is not caused by an insufficient density of grid points: the density is high enough at $\beta=0.6$. This drop of accuracy is due to the fact that the absorbing potential is situated at relatively short internuclear distances (from 20 to 40 a.u.). Exponentially decaying tails of excited vibrational wave functions reach this region. Therefore, the tails of these wave functions are not properly represented. Shifting the absorbing potential toward large distances would improve the accuracy, but it would require longer calculations. The accuracy of the predissociation rates is also limited by this fact. It is around 1–3%. However, for the purpose of the present study, such accuracy is largely sufficient.

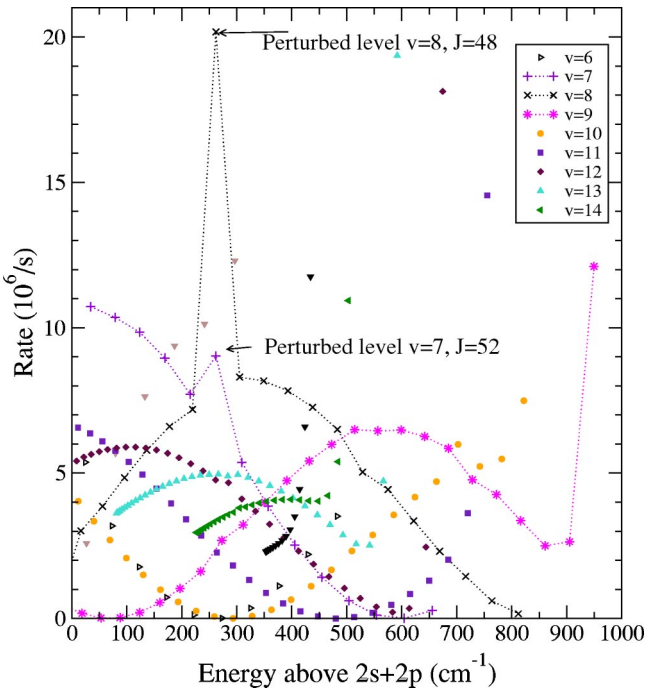

FIG. 4. Calculated predissociation rates of the $B\,^1\Pi_u$ levels. The rates show almost the same behavior as in the two-state calculation of Ref. [11], except two perturbations that are produced by accidental interactions with the $2\,^1\Sigma_g^+$ levels.

IV. RESULTS

A. Perturbed predissociation rates of $B\,^1\Pi_u$ rovibrational levels

Calculated predissociation rates of $B\,^1\Pi_u$ rovibrational levels are shown in Fig. 4. For clarity, the figure shows only $B\,^1\Pi_u$ rovibrational levels; the rates of $2\,^1\Sigma_g^+$ levels are not shown. As one can see, they essentially display the same behavior as in the two-state calculation of Ref. [11]. Two levels ($v=7$,$J=52$) and ($v=8$,$J=48$) clearly exhibit perturbations, as observed in the experiment. Experimental rates for the corresponding levels are 15×10^6 s^{-1} and 32×10^6 s^{-1}, the calculated ones being smaller, 10×10^6 s^{-1} and 20×10^6 s^{-1}, respectively. No significant change is observed in the calculated rates for the ($v=9$,$J=50$) level, although it is observed in the experiment. We attribute this disagreement to an insufficient knowledge of the $2\,^1\Sigma_g^+$ potential used in the calculation. For this level, the Franck-Condon overlap between a continuum wave function of the $1\,^1\Pi_g$ state and a corresponding wave function of the $2\,^1\Sigma_g^+$ level is very small. In principle, by appropriate fitting of the $2\,^1\Sigma_g^+$ potential near the barrier, one could obtain a more favorable Franck-Condon overlap, and therefore better agreement between experimental and theoretical rates.

A change of $B\,^1\Pi_u$ predissociation rates due to the presence of nearby $2\,^1\Sigma_g^+$ levels can be described qualitatively by considering wave functions of $B\,^1\Pi_u$, $1\,^1\Pi_g$ and $2\,^1\Sigma_g^+$ levels. The situation is demonstrated in Fig. 5, where the three-component wave function of the $^1\Pi_u(v=8,J=48)$ level is plotted. The maximum amplitude of the $1\,^1\Pi_g$ continuum component is 0.0018, instead of 0.0011 without a

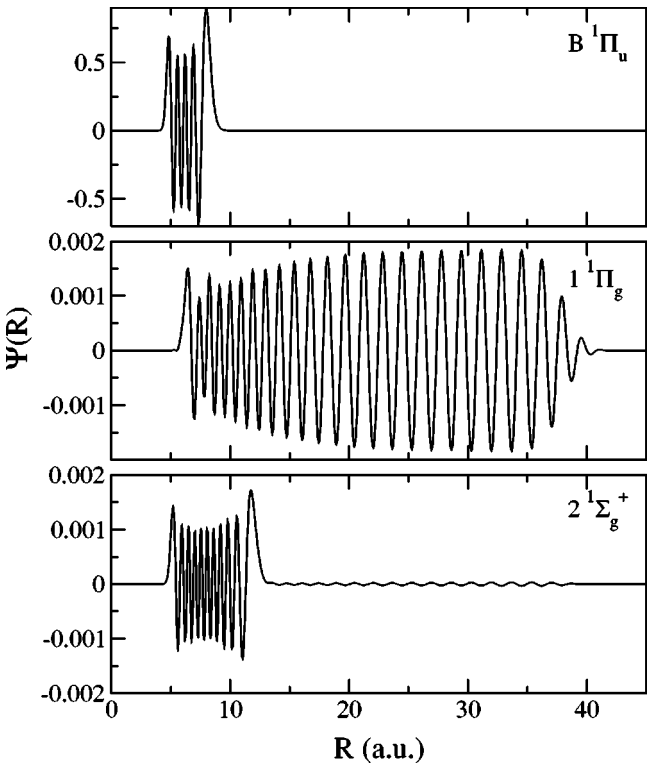

FIG. 5. The wave function of the $B\,^1\Pi_u(v=8,J=48)$ predissociated level. Because of the interaction with two other molecular states, the wave function has three components. The continuum component on the $1\,^1\Pi_g$ state (middle panel) is oscillating at large distances up to $R=40$ a.u., where an absorbing optical potential is used in our numerical calculations. The interaction between $1\,^1\Pi_g$ and $2\,^1\Sigma_g^+$ states enhances the amplitude of the $1\,^1\Pi_g$ continuum wave function. This turns into a corresponding increase of the Franck-Condon overlap between wave functions of the $1\,^1\Pi_g$ and $B\,^1\Pi_u$ levels and, therefore, to a higher predissociation rate.

coupling with the $2\,^1\Sigma_g^+$ state. The corresponding increase in dissociation rate relative to a two-state calculation is described by $(0.0018/0.0011)^2=2.7$.

Since the accuracy of the $2\,^1\Sigma_g^+$ potential used in the present calculation is probably not sufficient to reproduce exactly the energy positions of quasibound $2\,^1\Sigma_g^+$ levels within few wave numbers, we have tried to determine how sensitive are the perturbations to small modifications of the potential curve. For this goal, we have artificially modified the barrier of the $2\,^1\Sigma_g^+$ potential. As a result, energies of the $2\,^1\Sigma_g^+$ levels vary relatively to their $B\,^1\Pi_u$ partners. Figure 6 shows dependences of predissociation rates of the three $B\,^1\Pi_u$ e levels vs the energy difference between the $2\,^1\Sigma_g^+$ and $B\,^1\Pi_u$ levels. The three dependencies show a strong resonant character and reach zero at a certain energy difference, leading to a cancellation of predissociation. It can be noticed that the behavior of the rate curve for the $B\,^1\Pi_u(v=9,J=50)$ level is quite different from two other curves; the $^1\Pi_u(v=9,J=50)$ curve displays a very narrow resonance. The dependences shown in Fig. 6 can be interpreted using theory of Beutler-Fano profiles (see, for example, Refs. [19,20]), which was initially developed for studying of autoionizing resonances in atoms.

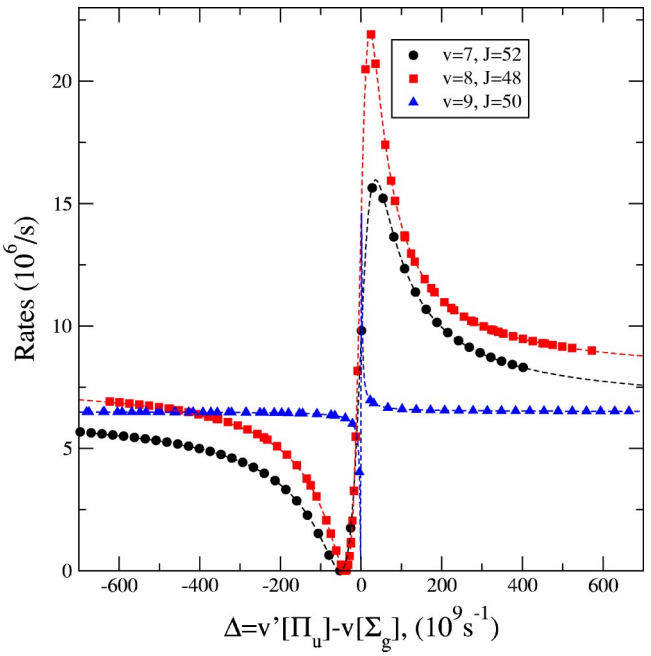

FIG. 6. Predissociation rates as functions of the energy difference between $B\,^1\Pi_u$ and $2\,^1\Sigma_g^+$ vibrational levels, shown by circles between $^1\Pi_u(v=7,J_e=52)$ and $^1\Sigma_g^+(v'=19,J=52)$, squares between $^1\Pi_u(v=8,J_e=48)$ and $^1\Sigma_g^+(v'=20,J=48)$, and triangles between $^1\Pi_u(v=9,J_e=50)$ and $^1\Sigma_g^+(v'=22,J=50)$. 100 10^9 s^{-1} corresponds to 0.53 cm^{-1}.

The total predissociation rate Γ_T of a given $B\,^1\Pi_u$ vibrational level v_u due to the coupling h_{ug} with the $1\,^1\Pi_g$ state can be represented by the familiar formula

$$\Gamma_T = 2\pi\langle\psi^{pert}_{\Pi_g}|h_{ug}|\psi_{\Pi_u}\rangle^2 \tag{5}$$

where ψ_{Π_u} is the wave function of the bound v_u level with energy E, calculated with no coupling between the $1\,^1\Pi_g$ and $B\,^1\Pi_u$ states; $\psi^{pert}_{\Pi_g}$ is the wave function of the $1\,^1\Pi_g$ continuum calculated at the same energy E. In standard theory of Feshbach resonances, the continuum wave function has a weak dependence on energy E. This is not true in the present case, since the continuum level is perturbed by a nearby $2\,^1\Sigma_g^+$ vibrational level v_g at energy $E_g=E-\Delta$, giving $\psi^{pert}_{\Pi_g}$ a strong energy dependence. The formalism of Beutler-Fano profiles can be adapted to the present case to describe this dependence in terms of a few parameters. For that purpose, we consider the width Γ_T in Eq. (5) as a square of a matrix element $\sqrt{2\pi}\langle\psi^{pert}_{\Pi_g}|h_{ug}|\psi_{\Pi_u}\rangle$ of the operator $\sqrt{2\pi}h_{ug}$ between an "initial" ψ_{Π_u} state and a "final" $\psi^{pert}_{\Pi_g}$ state and follow the derivation of Ref. [20] [see Eqs. (3.60)–(3.71) in Ref. [20]]. In order to adapt the treatment to the present case, we only have to replace the dipole moment operator $2\mu\omega\hat{r}$ by the operator $\sqrt{2\pi}h_{ug}$. The final formula reads

TABLE I. Parameters Q, Γ_u, and Γ_g obtained from the fit of the dependencies $\Gamma_T(E)$ to the analytical formula of Eq. (5) and from direct calculation of predissociation rates Γ_u and Γ_g. The agreement is very good, confirming the interpretation. A different behavior of the curve $\Gamma_T(E)$ for the pair $v_u=9$, $v_g=22$ is due to a relatively low Γ_g value.

Parameter	Γ_u, 10^6 s^{-1} (Fit)	Γ_u, 10^6 s^{-1} (Calculated)	Γ_g, 10^9 s^{-1} (Fit)	Γ_g, 10^9 s^{-1} (Calculated)	Q
$v_u=7$, $v_g=19$	6.61	6.54	85.56	92.1	1.19
$v_u=8$, $v_g=20$	7.87	7.89	59.4	58.5	1.34
$v_u=9$, $v_g=22$	6.50	6.46	1.23	3.84	1.32

$$\Gamma_T(E)=\Gamma_u\frac{(Q+\epsilon)^2}{1+\epsilon^2}, \tag{6}$$

where

$$\epsilon=\frac{E-E_g}{\Gamma_g/2}=\frac{\Delta}{\Gamma_g/2} \tag{7}$$

is a reduced energy. The parameters Γ_g and Γ_u have a simple physical interpretation. Γ_g is the width of a corresponding $2\,^1\Sigma_g^+$ predissociated level v_g in absence of the h_{ug} coupling, i.e., it can be represented as

$$\Gamma_g=2\pi\langle\psi_{\Sigma_g}|b\frac{\sqrt{J(J+1)}}{2\mu R^2}|\psi_{\Pi_g}^{nonpert}\rangle^2, \tag{8}$$

where ψ_{Σ_g} is an unperturbed wave function of the v_g level, and $\psi_{\Pi_g}^{nonpert}$ is the unperturbed (both, h_{ug} and JL, couplings are set to be zero) continuum wave function of the state Π_g. The width Γ_u is related to the predissociation of $B\,^1\Pi_u$ vibrational levels when JL coupling is neglected, i.e.,

$$\Gamma_u=2\pi\langle\psi_{\Pi_u}|h_{ug}|\psi_{\Pi_g}^{nonpert}\rangle^2, \tag{9}$$

where ψ_{Π_u} is the wave function of the corresponding $B\,^1\Pi_u$ level. When both perturbations are simultaneously introduced, the total width of the v_u level is described by Eq. (5).

The analytical formula (5) can be tested fitting the dependencies of total predissociation rates for the three v_u given in Fig. 6. It is clear from the figure that the variation of widths obtained by varying the energy difference Δ follows closely this analytical formula. The shape of the curves for the various v_u is determined by a variation of the rotational coupling matrix element yielding different values for the Γ_g widths. Table I gives the fitted values for the parameters Q, Γ_u, and Γ_g and compares them with values calculated directly. (Rates Γ_g can be directly calculated as described below.) Obtained analytical curves are represented in Fig. 6 by dashed lines. As one can see, the agreement between calculated and analytical dependencies for $\Gamma_T(E)$ is very good. The parameter Γ_u controls the overall amplitude of the curve, $\Gamma_T(E)$, Q controls the shape of the curve, and Γ_g determines the width.

Numerically, we have also investigated the effect of the rotational coupling on the shape of the resonant curves. For this goal we have reduced the magnitude of the rotational coupling and have again calculated the dependence of the predissociation rate as a function of the energy difference between the two interacting levels $^1\Pi_u(v=8,J=48)$ and $^1\Sigma_g^+(v=20,J=48)$. The result of this calculation is given in Fig. 7. The reduction of the coupling by a factor of 2 does not change the general form of the resonant curve but it does change the overall width by a factor of 4, which is in agreement with the previous discussion.

B. Λ-doubling of Li_2 $1\,^1\Pi_g$ bound levels

In order to check the validity of our calculation, we have applied our model to interpret experiment results of Linton *et al.* [16]. In their experiment, the effect of the Λ doubling

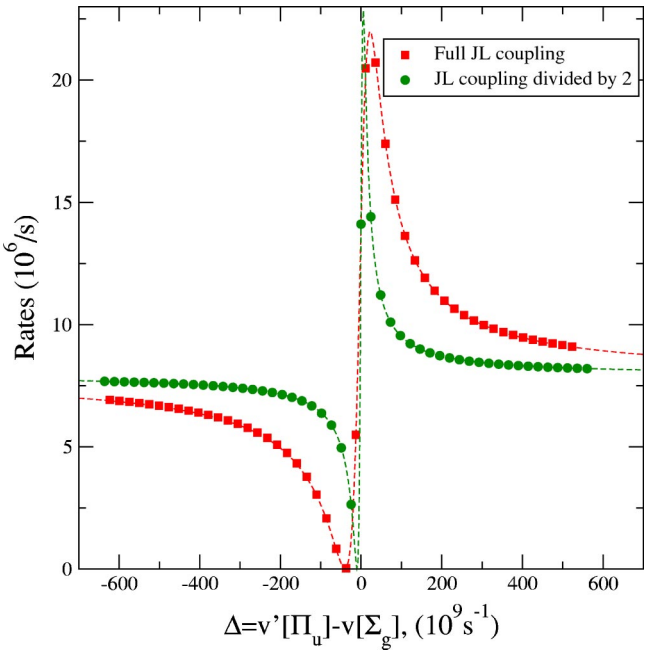

FIG. 7. The effect of a reduced coupling between $1\,^1\Pi_g$ and $2\,^1\Sigma_g^+$ molecular states on the predissociation rate of the $^1\Pi_u(v=8,J=48)$ level. We have modified the $^1\Sigma_g^+$ potential curve to produce a variable difference in energy between the $^1\Pi_u(v=8,J=48)$ and $^1\Sigma_g^+(v=20,J=48)$ levels. Squares show calculation for the actual rotational coupling, circles represent a calculation for a coupling twice smaller. The fitted parameters Q, Γ_u, and Γ_g for the last curve are 1.38, 7.91×10^6 s^{-1}, and 14.28×10^9 s^{-1}, respectively. The parameters for the former curve are given in Table I.

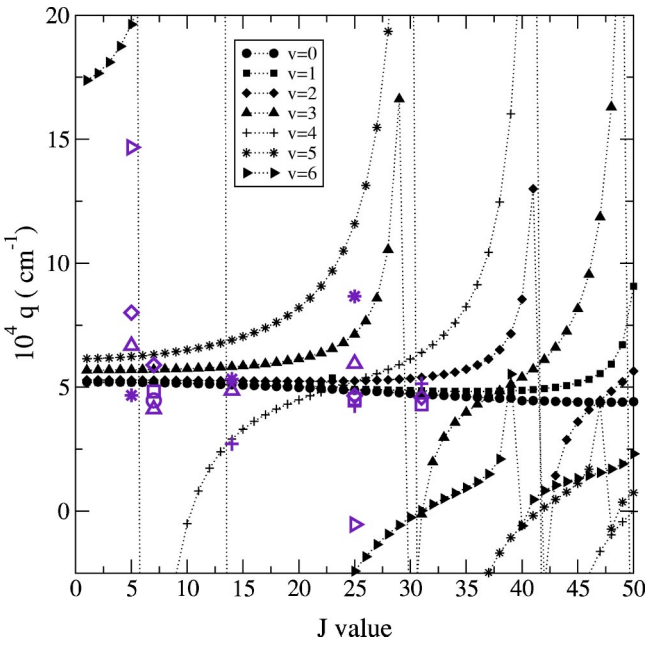

FIG. 8. Λ-doubling of several vibrational $1\,^1\Pi_g$ levels as a function of the total angular momentum J for the $^6Li_2$ molecule. Open gray symbols are experimental data [12].

of $1\,^1\Pi_g$ bound levels has been observed in homonuclear molecules $^6Li_2$ and $^7Li_2$. Therefore, $h_{ug}=0$ for this case.

Let us recall briefly the origin of the Λ-doubling. In the absence of the rotational coupling between the $2\,^1\Sigma_g^+$ and $1\,^1\Pi_g$ states in Eq. (4), $1\,^1\Pi_g$ rovibrational levels would be doubly degenerate (e and f parities). This parity is linked to symmetry with respect to a plane containing the molecular axis. In presence of rotational coupling, e parity levels of $1\,^1\Pi_g$ are coupled to $2\,^1\Sigma_g^+$ levels, the degeneracy is broken, and causes an energy splitting between e and f $1\,^1\Pi_g$ levels. The actual form of the coupling between $2\,^1\Sigma_g^+$ and $1\,^1\Pi_g$ makes the Λ-doubling varying linearly with $J(J+1)$. Therefore, it is convenient to represent the splitting ΔE between two $1\,^1\Pi_g$ levels [12] as

$$\Delta E = qJ(J+1), \tag{10}$$

where the parameter q is expected to depend weakly on J. An important advantage of the present method relies in its ability to treat the Λ-doubling globally, but not locally, as it was treated in Ref. [16].

In order to calculate the Λ-doubling, we have diagonalized the Hamiltonian including two molecular states: $2\,^1\Sigma_g^+$ and $1\,^1\Pi_g$ [see Eq. (4)]. Then, the Λ-doubling is determined as a shift in energy of a $1\,^1\Pi_g$ rovibrational level with respect to the energy of the same level in absence of the coupling between $2\,^1\Sigma_g^+$ and $1\,^1\Pi_g$.

As an example, Fig. 8 shows the calculated parameters q for several vibrational levels of the $^6Li_2$ molecule as a function of J. For the most of rovibrational levels, q is almost constant as expected. However, each rotational series of a given vibrational level shows a resonantlike behavior in some regions of J. These strong variations in q occur when a $2\,^1\Sigma_g^+$ level approaches very closely a given $1\,^1\Pi_g$ level. The amplitude of the variation is determined by a corresponding Franck-Condon overlap between the vibrational $1\,^1\Pi_g$ and $2\,^1\Sigma_g^+$ wave functions. Compared with a perturbation method, where every individual Λ-splitting is obtained as a sum over all the vibrational $2\,^1\Sigma_g^+$ levels located below and above the considered $1\,^1\Pi_g$ level, the present method provides the Λ-doubling for all vibrational levels in one single diagonalization. The experimental data of Linton *et al.* [16] are shown in Fig. 8 as open symbols. The agreement is satisfactory although not perfect. The comparison is also presented in Table II for both molecules $^6Li_2$ and $^7Li_2$. For the completeness of the table, we give also values of q obtained in the mentioned perturbation model of Ref. [16]. Since the energy positions of $2\,^1\Sigma_g^+$ and $1\,^1\Pi_g$ bound levels are determined in the experiment very accurately, the origin of the discrepancy between theory and experiment should is attributed to the present theoretical model. One possibility could be the employed approximation [Eq. (3)] of the rotational coupling. By a small change of the constant b from its approximated value of 2, a better agreement between the experimental data and calculations could be obtained. In this case, b should be considered as fitted to the experiment.

C. Predissociation rates of $2\,^1\Sigma_g^+$ levels

Predissociation rates of $2\,^1\Sigma_g^+$ rovibrational levels have never been observed experimentally for neither homonuclear nor heteronuclear isotopomers. In the perspective of experimental measurements, we have calculated these rates in the framework of our model including only two coupled $2\,^1\Sigma_g^+$ and $1\,^1\Pi_g$ channels (no u-g symmetry breaking is considered there). Results of the calculation are presented in Fig. 9 for $^6Li^7Li$. Similar to the u-g symmetry-breaking calculations, all rotational series for a given vibrational quantum number show different behaviors in two energy regions. At low energies, the rates display an oscillatory behavior determined by the Franck-Condon overlap between discrete and continuum wave functions. At larger energies, the rates grow exponentially due to the dominant tunneling effect. However, there is one qualitative difference from the case of interacting $B\,^1\Pi_u$ and $1\,^1\Pi_g$ molecular states. In contrast with the u-g symmetry-breaking calculations, the minima for all rotational series in Fig. 9 are located at the same energy around 400–450 cm^{-1}. Of course, if the u-g symmetry-breaking term is added, we return to our three coupled states calculation and the predissociation rates of $2\,^1\Sigma_g^+$ levels may exhibit some extra accidental perturbations. In the figure, we have marked the levels that are involved in the three perturbations considered above. The $(v'=19, J=48)$ and $(v'=20, J=52)$ quasi bound $2\,^1\Sigma_g^+$ levels coupled with the $1\,^1\Pi_g$ continuum are located near the maximum of the first part of the curve (maximum Franck-Condon overlap). The dissociation rate of the third $(v'=22, J=50)$ $2\,^1\Sigma_g^+$ level is almost ten times smaller because of an unfavorable Franck-Condon overlap between the corresponding wave functions. In this region dissociation by tunneling is not yet effective. This observation provides an insight into how one can improve agreement between theory and experiment for the third

TABLE II. Comparison of calculated and measured values of the Λ-doubling for $^6Li_2$ and $^7Li_2$. The strengths of the Λ-doubling are given in terms of the parameter $(10^4)q$ in cm^{-1} [16]. The upper number for each rovibrational level is the experimental value from Ref. [16], the middle number is the calculated value from Ref. [16], the lowest number (in bold) is the result of the present work.

	$^6Li_2$					$^7Li_2$			
v	$J=5$	7	14	25	31	17	19	38	40
0		4.46							
		2.56							
	5.20	**5.18**	**5.10**	**4.87**	**4.71**				
1		4.82		4.52	4.31				
		2.58		2.45	2.43				
	5.18	**5.17**	**5.10**	**4.91**	**4.85**				
2	8.00	5.89		4.65	4.58				3.64
	2.64	2.64		2.62	2.69				2.52
	5.29	**5.28**	**5.25**	**5.25**	**5.39**				**4.25**
3	6.67	4.11	4.86	5.95					3.20
	2.86	2.86	2.92	3.65					2.44
	5.70	**5.71**	**5.83**	**7.1**	**−0.12**				**3.81**
4			2.71	4.23	5.14	3.20			
			1.52	2.64	3.11	1.71			
	87.7	**−13.3**	**2.90**	**5.23**	**6.39**	**2.98**			
5	4.67		5.33	8.66		4.22			
	3.15		3.49	6.04		3.06			
	6.23	**6.31**	**6.90**	**11.6**	**−33**	**5.22**			
6	14.67			−0.54				1.11	
	10.55			−1.32				0.44	
	19.6	**22.5**	**−78.6**	**−2.42**	**0.02**			**0.81**	
7			1.1			0.95	1.37	1.75	
			−0.05			0.13	0.30	0.82	
	−1.07	**−0.87**	**0.01**	**1.37**	**0.88**	**0.32**	**0.52**	**1.74**	
8	4.67		0.52				1.16		
	1.05		0.49				0.13		
	1.69	**1.76**	**0.71**	**2.06**	**2.44**		**0.55**		
9							2.66		
							1.59		
							2.75		
10							−1.13		
							−1.65		
							−2.23		
11							2.34		
							1.30		
							2.35		
12							0.29		
							−0.34		
							0.42		

perturbation arising due to the interaction between $(v=9,J=50)$ $B\,^1\Pi_u^+$ and $(v'=22,J=50)$ $2\,^1\Sigma_g^+$ levels. The calculated rate Γ_g is small for the level $(v'=22,J=50)$ $2\,^1\Sigma_g^+$, it translates into a narrow width of the dependence $\Gamma_T(E)$ (see Fig. 6). In the experiment it is quite unlikely that two levels $(v_g'=22,J=50)$ and $(v_u=9,J=50)$ approach so closely. This suggests that the potential $2\,^1\Sigma_g^+$ should be modified in such a way that it would give a larger predissociation rate for the level $(v_g'=22,J=50)$.

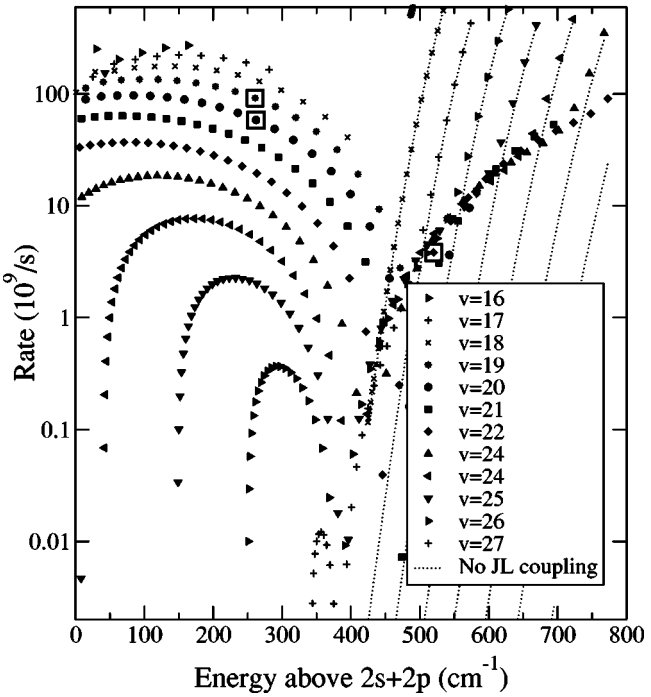

FIG. 9. Dissociation rates of $2\,^1\Sigma_g^+$ rovibrational levels of $^6Li^7Li$, calculated in the two-state model. Only the $2\,^1\Sigma_g^+$ and $1\,^1\Pi_g$ molecular states are included.

V. CONCLUSION

In the present study, we have considered accidental perturbations of predissociation rates of $B\,^1\Pi_u$ $^6Li^7Li$ quasibound levels, recently observed in a sub-Doppler experiment [11]. The data were first explained by *u-g* symmetry breaking and the coupling of the $B\,^1\Pi_u$ state with the continuum of the $1\,^1\Pi_g$ state. This two-state model, developed in the framework of the mapped Fourier grid method, allowed us to describe almost the whole set of experimental data except three perturbations. We have interpreted the perturbations as due to an indirect coupling of the $B\,^1\Pi_u$ state with a third molecular state, $2\,^1\Sigma_g^+$, which also has a potential barrier and dissociates to $(2s+2p)$. In fact, $1\,^1\Pi_g$ continuum wave functions are significantly coupled to both $2\,^1\Sigma_g^+$ and $B\,^1\Pi_u$ quasibound levels and a relatively strong effective interaction between the $2\,^1\Sigma_g^+$ and $B\,^1\Pi_u$ levels occurs through this continuum, only when a $2\,^1\Sigma_g^+$ level approaches a $B\,^1\Pi_u$ level.

The second result, which validates our model, is the calculation of Λ-doubling in the $1\,^1\Pi_g$ spectrum of $^7Li_2$ and $^6Li_2$. Our calculation reproduces qualitatively well the variation observed in experimental data [16].

As a third result, we have calculated predissociation rates of $2\,^1\Sigma_g^+$ rovibrational levels located above the dissociation limit. The tunneling effect and the coupling with the $1\,^1\Pi_g$ continuum of *e* parity have been taken into account. Predissociation of these levels has never been observed experimentally.

Hopefully, future experimental studies will provide information needed to improve the $2\,^1\Sigma_g^+$ potential above the dissociation limit. At present time, the accuracy of our calculations is mainly limited by a poor accuracy of this potential.

Our treatment represents an illustration of a more general situation where two closed channels are coupled via a third open channel. In our specific situation, numerical calculations show that resonance curves exhibit different types of behaviors (Fig. 6), which is interpreted using theory of Beutler-Fano profiles.

ACKNOWLEDGMENT

We would like to thank Philippe Durand for discussions about a possible approach of treatment of the three-state system using analytical methods.

[1] I. Russier, F. Martin, C. Linton, P. Crozet, A.J. Ross, R. Bacis, and S. Churassy, J. Mol. Spectrosc. **168**, 39 (1994).
[2] H. Richter, H. Knöckel, and E. Tiemann, Chem. Phys. **157**, 217 (1991).
[3] J. Heinze, P. Kowalczyk, and F. Engelke, J. Chem. Phys. **89**, 3428 (1988).
[4] J.X. Wang, H. Wang, P.D. Kleiber, A.M. Lyyra, and W.C. Stwalley, J. Phys. Chem. **95**, 8040 (1991).
[5] C. Amiot and J. Vergès, Chem. Phys. Lett. **274**, 91 (1997).
[6] P. Cacciani and V. Kokoouline, Phys. Rev. Lett. **84**, 5296 (2000).
[7] Á. Vibók and G.G. Balint-Kurti, J. Phys. Chem. **96**, 8712 (1992); Á. Vibók and G.G. Balint-Kurti, J. Chem. Phys. **96**, 7615 (1992); M. Monnerville and J.M. Robbe, Eur. Phys. J. D **5**, 381 (1999).
[8] O. Dulieu and P.S. Julienne, J. Chem. Phys. **103**, 60 (1995).
[9] V. Kokoouline, O. Dulieu, R. Kosloff, and F. Masnou-Seeuws, J. Chem. Phys. **110**, 9865 (1999).
[10] V. Kokoouline, O. Dulieu, R. Kosloff, and F. Masnou-Seeuws, Phys. Rev. A **62**, 032716 (2000).
[11] N. Bouloufa, P. Cacciani, V. Kokoouline, F. Masnou-Seeuws, R. Vetter, and Li Li, Phys. Rev. A **63**, 042507 (2001).
[12] N. Bouloufa, P. Cacciani, R. Vetter, A. Yiannopoulou, F. Martin, and A.J. Ross, J. Chem. Phys. **114**, 8445 (2001).
[13] I. Schmindt-Mink, W. Müller, and W. Meyer, Chem. Phys. **92**, 263 (1985).
[14] B. Barakat, R. Bacis, S. Churassy, R.W. Field, J. Ho, C. Linton, S. McDonald, F. Martin, and J. Vergès, J. Mol. Spectrosc. **116**, 271 (1986).
[15] C. He, L.P. Gold, and R.A. Bernheim, J. Chem. Phys. **95**, 7947 (1991).
[16] C. Linton, F. Martin, R. Bacis, and J. Vergès, J. Mol. Spectrosc. **142**, 340 (1990).
[17] J. Cariou and P. Luc, *Atlas du Spectre d'Absorption de la Molécule de Tellure* (Laboratoire Aimé Cotton, Orsay, France, 1980).
[18] H. Lefebvre-Brion and R. W. Field, *Perturbations in the Spectra of Diatomic Molecules* (Academic Press, London, 1986).
[19] U. Fano and A. R. P. Rau, *Atomic Collisions and Spectra* (Academic Press, Orlando, FL, 1986).
[20] H. Friedrich, *Theoretical Atomic Physics* (Springer, New York, 1998).